Genes, Brain and Behavior (2003) **2:** 238–252

ISSN 1601-183X

Genetic architecture of the mouse hippocampus: identification of gene loci with selective regional effects

J. L. Peirce, E. J. Chesler, R. W. Williams and L. Lu*

Center for Neuroscience, Department of Anatomy and Neurobiology, University of Tennessee Health Science Center, Monroe Avenue, Memphis, Tennessee, USA

**Corresponding author: L. Lu, Center for Neuroscience, Department of Anatomy and Neurobiology, University of Tennessee Health Science Center, 855 Monroe Avenue, Memphis, Tennessee 38163, USA. E-mail: lulu@nb.utmem.edu*

We recently mapped two quantitative trait loci that have widespread effects on hippocampal architecture in mouse: *Hipp1a* and *Hipp5a*. We also noted remarkable strain differences in the relative sizes of different hippocampal regions. Estimated heritable variation for these differences was 42% in hippocampus proper, 40% in dentate gyrus, 31% in granule cell layer and 18% in pyramidal cell layer. Region size varied at least 50% from largest to smallest measurement. Here we have utilized these differences to identify loci with effects on the dentate gyrus, granule cell layer, hippocampus proper and pyramidal cell layer. Our sample consists of C57BL/6J and DBA/2J and 32 BXD recombinant inbred strains. Volumetric data were corrected for shrinkage and for differences in brain weight. We identified significant loci on chromosomes (Chr) 6, 13 and 15, and a significant interaction locus on proximal Chr 11. A suggestive distal Chr 1 locus overlaps with *Hipp1a*. *HipV13a* (Chr 13, 42–78 Mb) has an additive effect of 0.56 mm^3 (12.1%) on dentate gyrus volume, while *GrV6a* (Chr 6, 29–65 Mb) has additive effects of 0.14 mm^3 (16.0%) on the volume of the granule cell layer. *HipV13a* also interacts with *DGVi11a*, a locus on proximal Chr 11 that operates exclusively through its epistatic effect on *HipV13a* and has no independent main effect. *HipV15a* (Chr 15, 0–51 Mb) has an additive effect of 1.76 mm^3 (9.0%) on the volume of the hippocampus proper. We used WebQTL, a recently described web-based tool, to examine genetic correlation of gene expression with hippocampal volume. We identified a number of genes that map within the QTL intervals and have highly correlated expression patterns. Using WebQTL's extensive database of published BXD phenotypes, we also detected a strong and potentially biologically meaningful correlation between hippocampal volume and the acoustic startle response.

Keywords: BXD recombinant inbred strain, C57BL/ 6J, complex trait analysis, DBA/ 2J, heritability, mouse brain, quantitative trait locus (QTL), spatial memory

Received 14 December 2002, revised 17 June 2003, accepted for publication 17 June 2003

We recently applied complex trait analysis to explore the genetic basis of the marked structural and functional variation in the mouse hippocampus. We uncovered two quantitative trait loci (QTL); *Hipp1a* and *Hipp5a*, each of which has specific effects on the overall size and weight of the mouse hippocampus (Lu *et al*. 2001). These loci map to Chrs 1 and 5, in intervals that have been narrowed using a combination of recombinant inbred (RI) strains and an F2 intercross to about 15 cM. Both loci alter total hippocampal weight, volume and cell number over a range of 10–20%, an effect size greater than that associated with age or sex in laboratory mice (Abusaad *et al*. 1999; Lu *et al*. 2001). Effects of the initial *Hipp* loci are widespread and known to extend to multiple hippocampal regions.

However, the architecture of the hippocampus involves both global and regional controls. Confirming early work by Wimer *et al*. (1976, 1978), we noted remarkable strain variation in the relative sizes of different hippocampal regions. For example, we found that the volume of the granule cell layer and pyramidal cell layer varies as much as 30% between several pairs of inbred strains that have almost the same overall hippocampal size. This finding raised the intriguing possibility of mapping QTL that have specific effects on different regions of the hippocampus. In the present work, we have focused on refining our understanding of hippocampal size variation by dissecting genetic variance in the volumes of several distinct regions that make up the hippocampus. Our intent was to discover novel QTL with restricted effects on particular hippocampal regions in RI strains derived from a cross between C57BL/6J and DBA/ 2J (BXD). Since the structure and function relationships of hippocampal regions have been a subject of intense study for some time (reviewed in Crusio 2001 (mossy fibers); Deadwyler *et al*. (1987) (sensory input); Kesner *et al*. 2000 (models of regional function) and others) investigation of

these strain differences may serve to provide insight into behavioral variations in hippocampus-dependent phenotypes.

Examination of hippocampal structure using complex trait analysis complements the sophisticated array of methods currently being used to explore gene function and expression in the hippocampus. For instance, genetic perturbations of CREB protein (Gass *et al*. 1998; Graves *et al*. 2002), NMDA receptors (reviewed in Shapiro 2001; Wittenberg & Tsien 2002), RXRG (Chiang *et al*. 1998), and NGF (Ruberti *et al*. 2000) in mice have highlighted the critical role of these proteins in spatial memory and learning. Expression profiling now also broadens the range of molecules that can be screened for involvement in hippocampal function to a large fraction of the entire genome (Pavlidis & Noble 2001). Localization of genetic factors modulating regionally defined variation in hippocampus size complements our increasing biochemical understanding of the workings of this important CNS structure.

Materials and methods

A set of 32 BXD/Ty RI strains and parental strains C57BL/6J (B6) and DBA/2J (D2) were used for both QTL mapping and biometric analysis of the hippocampus and its component regions. The BXD RI strains were generated by crossing C57BL/6J (B6) and DBA/2J (D2) parental strains in the mid-1970s (BXD1 through 32) and 1990s (BXD33 through 42) by Taylor 1989, 1999). RI strains are completely inbred lines derived from brother-sister matings starting from an F2 intercross. Parental and RI mice analyzed here are part of the Mouse Brain Library (http://www.mbl.org/) (MBL), and serial sections for all animals described are available on the MBL web site. Animal husbandry and section preparation for animals in this data set are described below. All phenotype data and additional supplemental data will be made available online at ftp://atlas.utmem.edu/public/.

Animal husbandry and age

Mice were maintained at 20–24 °C on a 14/10 h light/dark cycle in a pathogen-free colony at the University of Tennessee. All animals were fed 5% fat Agway Prolab 3000 (Agway Inc., Syracuse, NY) rat and mouse chow. The average age of BXD/Ty animals at time of sacrifice was 87 days with a range of 38–359 days.

Fixation and sectioning

Mice were deeply anesthetized with Avertin (1.25% 2,2,2-tribromoethanol and 0.8% tert-pentyl alcohol in water, 0.5–1.0 ml intraperitoneal injection). They were then perfused through the heart with 0.1 M phosphate buffered saline followed by 1.25% glutaraldehyde and 1.0% (in a few cases 4%) paraformaldehyde in 0.1 M phosphate buffer, and then by 2.5% glutaraldehyde and 2.0% paraformaldehyde in 0.1 M buffer. Brain tissue was subsequently embedded in celloidin. Sections were taken at approximately 30 μm thickness using a sliding microtome and stained using cresyl violet. Plane of sectioning was also noted, since we have previously observed (unpublished data) that even in well matched sets of animals there is a small but consistent difference in measured volume between coronally and horizontally sectioned animals. However, since the effect is quite small, we did not attempt to model it. Additional details are available at http://www.mbl.org/tutorials/MBLTraining-Manual/index.html.

Volumetric measurement of the hippocampus

We analyzed section images from a set of 32 BXD strains and the two parental strains to identify QTL modulating hippocampal volume and to analyze potential regional effects on the dentate gyrus, including the granule cell layer, the hippocampus proper, including the pyramidal cell layer, and the total hippocampus. Images of the serial sections through the entire hippocampus from 232 BXD cases (average of 5 per strain), 8 B6 cases and 6 D2 cases were downloaded from http://www.mbl.org/ and analyzed in NIH IMAGE. Images were not available for BXD strains 6, 21 and 37. Serial section images have a physical resolution of 4.5 μm/pixel, and the interval between adjacent sections on each slide is 300 μm. Volume was determined by summing the area of each measured region in each image and multiplying by the section interval, typically with a set of 9–11 sections per hippocampus. For the granule cell layer and pyramidal cell layer, we also measured cell number in the sections examined and calculated the correlation.

Borders of the hippocampus, excluding the subiculum but including the fimbria (included for consistency with Lu *et al*. 2001) and dentate gyrus (Fig. 1) were traced manually, followed by manual tracing of the dentate gyrus alone. The area of the hippocampus proper was obtained by subtracting the area of the dentate gyrus from the total hippocampal area. Finally, areas of the pyramidal cell layer (CA1–CA3) in the hippocampus proper and the granule cell layer of the dentate gyrus were measured bilaterally for all cases. These layers have a high cell packing density and can be reliably defined by a thresholding operation in NIH Image, eliminating the need for manual tracing. To improve uniformity of the data set the last author conducted all thresholding. The reliability of thresholding was tested by repeated measures analysis, and correlation of duplicated estimates was extremely high ($r = 0.95$). Shrinkage among cases in the MBL is variable, but known. The celloidin embedding process typically shrinks tissues by a factor of 2.48 ± 0.25 to approximately $40.8\% \pm 4.1\%$ of initial volume. To correct for variance due to shrinkage caused by celloidin embedding, we divided hippocampal volumes by the total brain volume and then multiplied by the brain volume expected from the known brain weight, assuming a brain density of 1.05 mg per mm^3 of fixed tissue. The post-processing volume of the total brain was measured by point counting as described in Williams (2000).

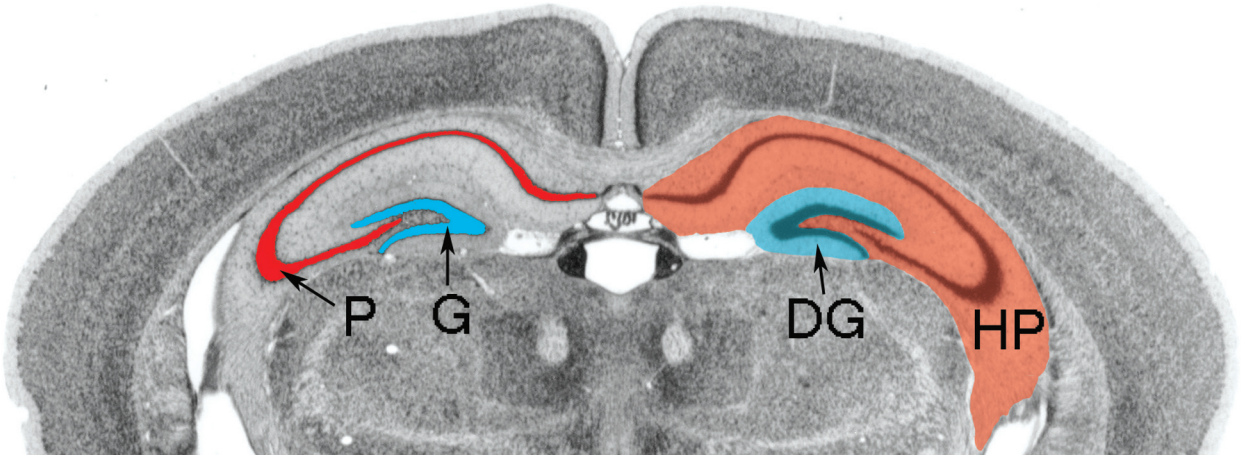

Figure 1: A typical hippocampus section. The hippocampus proper (HP) and dentate gyrus (DG) are shaded on the right, while the granule cell layer of the dentate gyrus (G) and the pyramidal cell layer of the hippocampus proper (P) are shaded on the left.

All volume data have been corrected for shrinkage, case-by-case. Volumetric data used in the results are group means based on 3–11 cases per strain.

Modeling hippocampal volume

We fit a simple regression relating brain weight and hippocampal volume to the data. Although this method may add a conservative bias against QTL detection, particularly in the probable event that brain weight interacts with the genetic factors we are interested in studying (Darlington & Smulders 2001), we felt it necessary to adjust for its relatively strong effect on hippocampal volume before QTL mapping. Regressions were generated for each hippocampal region using the simple regression function in EXCEL 97 (Microsoft Corporation, http://www.microsoft.com/). These regressions were used to generate predicted and residual values from our data set. We then performed QTL mapping as described below using the residual values. More complex general linear model (GLM) approaches were also explored, and the QTL discussed are consistent using these approaches as well (data available online at ftp://atlas.utmem. edu/public).

Genotyping and QTL mapping

Genomic DNA from BXD RI mice was extracted and genotypes were determined as described in Williams *et al.* (2001a). A set of 623 microsatellite loci distributed across all autosomes and the X-chromosome were used in all mapping and permutation analysis. Genotypes were entered into EXCEL 97 and transferred to MAP MANAGER QTX (QTX; Manly *et al.* 2001). Residuals generated from the models described above were exported from EXCEL 97 for analysis and mapping in QTX and WebQTL (http://www.webqtl.org/; Wang *et al.* in press). In order to examine whether or not our modeling of nuisance variables substantially changed the locations and identifications of our underlying QTL, we repeated interval mapping for all chromosomes using unmodified volume data collected as described above. Additionally, we mapped QTL for body weight and brain weight in our population and compared the locations of these QTL with the set of hippocampus volume QTL.

QTX and WebQTL both implement simple interval mapping methods described by Haley and Knott (1992), and QTX additionally implements composite interval mapping methods. Genome-wide significance levels for assessing confidence in linkage statistics were estimated by comparing the peak likelihood ratio statistic (LRS) of correctly ordered data sets with LRS computed for 10 000 permutations (Churchill & Doerge 1994). LRS scores can be converted to logarithm of the odds (LOD) scores simply by dividing by 4.6. In general, QTL modulating hippocampal volume in larger regions were considered first using WebQTL. Where appropriate, markers from discovered QTL were tested as controls in examination of increasingly specific regions of the hippocampus. After discovery of these individual QTL, QTX was used to determine whether there were any significant interactions. QTX tests each possible pair of markers for main and interaction effects. Naturally, the threshold for significance for such a test must be quite high. In this case marker pairs were only considered if they achieved a nominal $P < 10^{-5}$ for the marker pair and $P < 0.01$ for the interaction effect itself. Reported genome-wide significance was determined by computing at least 10 000 permutations.

Genetic correlations of hippocampal anatomy with gene expression

Genetic correlation analysis using phenotypic values of gene expression and anatomical traits in these isogenic mice is a novel hypothesis-generating approach to identifying potentially interesting genes that map within the QTL interval.

Expression data for the strains in the present study were selected from a larger set (Shou *et al.* 2002) generated using the Affymetrix U74Av2 (http://www.affymetrix.com/index.affx) array and made available via WebQTL. Using WebQTL, correlations with this forebrain expression data set were determined and ranked by correlation or position. Notably, WebQTL also facilitates correlation with other expression data sets and a variety of published phenotypes.

Expression measurements made by Shou and colleagues (2002) were based on at least four arrays per BXD or progenitor strain, and each array was generated from a tissue pool of three forebrain samples including hippocampus. Spearman's rank correlations were used to associate BXD strain phenotypes for hippocampal traits with transcript expression levels. From an initial set of the top 500 correlations between brain expression and hippocampal phenotypes, we selected those that reside in the QTL region and themselves have a transcriptional control QTL (Williams *et al.* 2002) in the same region. Where there were still a large number of correlated transcripts (Chr 1), we removed the least correlated transcripts and selected a manageable number to display here, giving priority to known genes. It is important to recognize that this approach is hypothesis generating as opposed to hypothesis limiting. Trait-relevant polymorphisms need not be manifest in expression level effects, though expression level differences are a likely source of QTL effects.

Results

Hippocampal volume of parental strains

Hippocampal volume of the parental strains B6 and D2 are $28.0 \pm 0.73\,mm^3$ and $24.3 \pm 0.47\,mm^3$, respectively. This 13.2% difference is highly significant ($P < 0.001$). Each hippocampal compartment that we examined is also larger in B6 than in D2, and in all but one case these differences are also statistically significant. The volumes of the hippocampus proper are $22.4 \pm 0.65\,mm^3$ and $19.7 \pm 0.37\,mm^3$, respectively, for the two strains ($P = 0.004$). Corresponding values for the dentate gyrus are $5.6 \pm 0.14\,mm^3$ and $4.6 \pm 0.13\,mm^3$ ($P < 0.001$), whereas those for the granule cell layer volume are $1.1 \pm 0.05\,mm^3$ and $0.75 \pm 0.02\,mm^3$ ($P < 0.001$). The pyramidal cell layer volume follows this same trend: $1.4 \pm 0.11\,mm^3$ and $1.2 \pm 0.06\,mm^3$, respectively ($P = 0.07$) (Table 1). Total brain weight of B6 animals is approximately 16% greater than that of D2 (477.4 ± 4.8 mg vs. 401.4 ± 5.6 mg). Body weight of B6 is approximately 9.4% greater than that of D2 (28.6 g vs. 25.9 g, Table 2). It is interesting to note that if hippocampal volume of the two strains is adjusted by linear regression to account for differences in both brain and body weight, then the differences in hippocampus proper, dentate gyrus and pyramidal cell layer volume between B6 and D2 are not statistically significant ($P > 0.05$).

Brain weight and hippocampal volume

In BXD mice, variation in brain weight (Table 2) is the single most important predictor of variation in hippocampal volume. Approximately 39% of variance in hippocampal proper volume ($F_{1,230} = 149$, $P < 0.0001$) is accounted for by brain weight. Brain weight also accounts for 31% of the variance in dentate gyrus volume ($F_{1,230} = 102$, $P < 0.0001$), 11% of variance in granule cell layer volume ($F_{1,230} = 29.6$, $P < 0.0001$) and 8.4% of variance in pyramidal cell layer volume ($F_{1,230} = 21.2$, $P < 0.0001$)

Body weight and hippocampal volume

Body weight (Table 2) also has a significant correlation with hippocampal proper volume ($r = 0.26$, df = 230, $P < 0.0001$) and dentate gyrus volume ($r = 0.27$, df = 230, $P < 0.0001$). In contrast, body weight has no significant correlation with pyramidal cell layer volume ($r = 0.06$, df = 230, $P = 0.41$) or granule cell layer volume ($r = 0.02$, df = 230, $P = 0.82$). An increase in body weight of 1 g is associated with an increase in the volume of the hippocampus proper of $0.14 \pm 0.03\,mm^3$ and dentate gyrus of $0.04 \pm 0.01\,mm^3$. While this effect is correlated with the effect of sex on hippocampal region volumes, the effect of body weight exceeds that attributable to the main effect of sexual dimorphism.

Brain weight and body weight

Unsurprisingly, body and brain weight are relatively correlated measures, and this correlation is highly significant ($r = 0.48$, df = 248, $P < 2 \times 10^{-16}$). The correlation is almost unchanged when brain weight is compared to body weight minus brain weight. ($r = 0.48$, df = 248, $P < 2 \times 10^{-15}$).

Age and hippocampal volume

The volume of the hippocampus proper and the dentate gyrus increases significantly as a function of age. Within our sample of BXD animals (averages, Table 2) that ranged in age from 36 to 359 days, the slopes of these increases are approximately 2.4 and $0.82\,mm^3$, respectively, for a 10-fold increase in age. Mice are sexually mature by 50 days of age, and over the next 200 days the summed volume of the hippocampal proper and dentate gyrus increase by 1.7 and $0.57\,mm^3$, respectively. Variation in age among BXD mice accounts for 4.5% of the variance in hippocampal proper volume ($F_{1,230} = 10.9$, $P = 0.001$) and 6.2% of the variance in dentate gyrus volume ($F_{1,230} = 15.1$, $P = 0.0001$). However, age is not an important predictor in either pyramidal cell layer volume ($F_{1,230} = 0.58$, $P = 0.45$) or granule cell layer volume ($F_{1,230} = 0.04$, $P = 0.83$).

Sex and hippocampal volume

We find that the volume of the total hippocampus and hippocampal regions in male mice is typically larger than the equivalent volume in female mice at the same age. The only exception is pyramidal cell layer volume. The male hippocampus proper is $0.7\,mm^3$ larger ($F_{2,229} = 7.8$, $P < 0.05$), the

Table 1: Original volume of hippocampal regions in BXD recombinant inbred strains

Strain	Samples	Hippocampus	Hippocampus proper	Pyramidal cell layer	Granule cell layer	Dentate gyrus
BXD1	11	28.4 ± 0.8	23.0 ± 0.6	1.68 ± 0.09	1.06 ± 0.03	5.44 ± 0.21
BXD2	6	22.4 ± 0.5	18.7 ± 0.4	1.42 ± 0.04	0.75 ± 0.03	3.74 ± 0.12
BXD5	5	26.7 ± 0.9	21.4 ± 0.7	1.60 ± 0.12	0.99 ± 0.07	5.31 ± 0.22
BXD8	8	28.0 ± 1.2	22.3 ± 1.0	1.69 ± 0.10	1.13 ± 0.05	5.71 ± 0.16
BXD9	8	22.5 ± 0.5	18.1 ± 0.4	1.38 ± 0.04	0.85 ± 0.03	4.39 ± 0.06
BXD11	6	25.7 ± 1.1	21.3 ± 0.8	1.60 ± 0.11	1.00 ± 0.12	4.45 ± 0.30
BXD12	8	25.3 ± 0.7	20.5 ± 0.6	1.58 ± 0.09	0.87 ± 0.04	4.72 ± 0.18
BXD13	8	23.7 ± 0.7	19.2 ± 0.6	1.46 ± 0.07	0.95 ± 0.05	4.52 ± 0.11
BXD14	6	24.6 ± 0.7	19.7 ± 0.6	1.61 ± 0.14	1.10 ± 0.06	4.95 ± 0.18
BXD15	5	27.0 ± 0.7	21.9 ± 0.5	1.58 ± 0.09	0.85 ± 0.05	5.17 ± 0.24
BXD16	3	22.7 ± 0.6	18.9 ± 0.7	1.37 ± 0.03	0.50 ± 0.03	3.86 ± 0.21
BXD18	7	24.5 ± 0.5	19.6 ± 0.4	1.55 ± 0.07	0.87 ± 0.02	4.86 ± 0.14
BXD19	8	27.4 ± 0.9	22.2 ± 0.6	1.74 ± 0.15	0.97 ± 0.04	5.25 ± 0.31
BXD20	5	21.7 ± 0.7	17.6 ± 0.7	1.16 ± 0.08	0.75 ± 0.04	4.05 ± 0.07
BXD22	7	26.8 ± 0.4	21.3 ± 0.3	1.49 ± 0.07	1.01 ± 0.06	5.47 ± 0.18
BXD23	8	23.6 ± 0.8	19.2 ± 0.7	1.44 ± 0.11	0.80 ± 0.04	4.35 ± 0.17
BXD24	8	23.6 ± 0.5	19.3 ± 0.4	1.47 ± 0.10	0.84 ± 0.05	4.39 ± 0.11
BXD25	8	22.5 ± 1.1	18.2 ± 0.8	1.43 ± 0.08	0.94 ± 0.08	4.30 ± 0.25
BXD27	8	20.4 ± 0.8	16.7 ± 0.7	1.33 ± 0.11	0.75 ± 0.08	3.70 ± 0.19
BXD28	8	21.3 ± 0.6	17.1 ± 0.5	1.33 ± 0.12	0.84 ± 0.06	4.21 ± 0.11
BXD29	8	20.4 ± 0.8	16.3 ± 0.7	1.15 ± 0.06	0.69 ± 0.05	4.07 ± 0.15
BXD30	7	18.9 ± 0.7	15.2 ± 0.5	1.24 ± 0.07	0.79 ± 0.06	3.74 ± 0.23
BXD31	6	23.7 ± 0.7	19.3 ± 0.5	1.43 ± 0.11	0.78 ± 0.07	4.37 ± 0.16
BXD32	8	26.6 ± 0.9	21.6 ± 0.8	1.48 ± 0.06	0.91 ± 0.04	4.94 ± 0.19
BXD33	8	21.6 ± 0.6	17.5 ± 0.5	1.39 ± 0.08	0.74 ± 0.03	4.13 ± 0.12
BXD34	8	20.5 ± 0.7	16.8 ± 0.5	1.38 ± 0.06	0.66 ± 0.04	3.69 ± 0.14
BXD35	8	23.0 ± 0.5	18.5 ± 0.3	1.38 ± 0.04	0.85 ± 0.04	4.55 ± 0.23
BXD36	8	23.6 ± 0.7	19.3 ± 0.5	1.46 ± 0.06	0.76 ± 0.05	4.30 ± 0.17
BXD38	6	24.1 ± 0.5	19.8 ± 0.4	1.64 ± 0.11	0.84 ± 0.03	4.38 ± 0.09
BXD39	8	22.2 ± 0.7	17.9 ± 0.6	1.23 ± 0.07	0.96 ± 0.04	4.23 ± 0.09
BXD40	8	27.4 ± 1.0	22.2 ± 0.8	1.65 ± 0.14	1.04 ± 0.09	5.19 ± 0.30
BXD42	8	25.4 ± 0.6	20.2 ± 0.4	1.48 ± 0.07	1.05 ± 0.05	5.20 ± 0.22
C57BL/6 J	9	28.0 ± 0.7	22.4 ± 0.6	1.41 ± 0.11	1.09 ± 0.05	5.63 ± 0.14
DBA/2 J	8	24.3 ± 0.5	19.7 ± 0.4	1.18 ± 0.06	0.75 ± 0.02	4.55 ± 0.13
Average	7.3	24.1 ± 0.7	19.5 ± 0.6	1.45 ± 0.09	0.87 ± 0.05	4.58 ± 0.17
Average (no parentals)	7.25	23.9 ± 0.7	19.4 ± 0.6	1.46 ± 0.09	0.87 ± 0.05	4.55 ± 0.17

Volumes are given in mm^3 as average ± standard error.

dentate gyrus is 0.23 mm^3 larger ($F_{2,229} = 10.6$, $P < 0.05$), and granule cell layer is 0.06 mm^3 larger ($F_{2,229} = 2.5$, $P < 0.05$) than that of female mice. Despite differences in body weight, male and female mice have almost the same brain weight: 423.4 ± 2.7 vs. 417.8 ± 4.2 mg, respectively ($t_{186} = 1.14$, $P = 0.26$). The difference in hippocampal volume is therefore at least partly a structure specific CNS sex difference. Although statistically significant, the difference in hippocampal volume between the sexes is relatively trivial given the numerous other sources of variance. Sex accounts for only about 2% of the total variance in hippocampal volume and approximately the same percentage of individual hippocampal regions. Substantial sex differences do exist in other inbred mouse strains (Wimer & Wimer 1985; 1989) and other mammalian species (Jacobs *et al*. 1990; Jacobs & Spencer 1994).

Comparison of right and left hippocampi

Any differences in volumes of right and left hippocampi are due to a combination of biological differences and technical error. The mean difference between the two sides averages 0.37 mm^3 in hippocampal proper volume, 0.12 mm^3 in dentate gyrus volume, 0.06 mm^3 in pyramidal cell layer volume and 0.05 mm^3 in granule cell layer volume. Following a correction for small *n*, these values correspond to a right-left coefficient of variation (CV) of 3.4% in hippocampal proper

Table 2: Average age, body weight and brain weight as well as frequency of sex and section type in sample

Strain	Males	Females	Coronal Section	Horizontal Section	Age (days)	Body Weight (g)	Brain Weight (mg)
C57BL/6	6	3	3	6	203.8 ± 40.0	28.6 ± 2.2	477.4 ± 4.8
DBA/2	5	3	3	5	234.8 ± 37.7	25.9 ± 1.3	401.4 ± 5.6
BXD1	8	3	6	5	51.7 ± 0.9	20.7 ± 1.2	458.0 ± 7.3
BXD2	3	3	2	4	61.3 ± 7.4	21.9 ± 1.5	426.6 ± 5.9
BXD5	1	4	3	2	205.4 ± 39.2	28.3 ± 0.6	544.9 ± 9.4
BXD8	6	2	5	3	179.0 ± 76.6	24.3 ± 1.5	424.8 ± 10.4
BXD9	3	5	3	5	92.9 ± 21.0	23.9 ± 1.8	434.9 ± 2.7
BXD11	3	3	3	3	62.2 ± 8.9	19.1 ± 1.9	429.0 ± 9.7
BXD12	5	3	5	7	98.6 ± 8.2	23.2 ± 1.4	438.4 ± 8.5
BXD13	5	3	4	4	68.3 ± 7.0	23.1 ± 1.3	417.7 ± 4.0
BXD14	2	4	3	3	89.6 ± 12.3	23.2 ± 1.4	444.4 ± 8.6
BXD15	2	3	3	2	150.4 ± 22.9	28.7 ± 0.7	453.1 ± 4.4
BXD16	1	2	0	3	56.0 ± 20.0	23.5 ± 1.3	435.6 ± 11.6
BXD18	4	3	4	3	90.7 ± 11.1	22.0 ± 1.9	418.0 ± 5.0
BXD19	4	4	4	4	103.3 ± 15.6	21.2 ± 1.4	425.4 ± 6.7
BXD20	3	2	2	3	95.8 ± 15.8	21.7 ± 1.6	392.2 ± 3.2
BXD22	3	4	4	3	128.1 ± 22.2	25.5 ± 2.4	458.2 ± 6.5
BXD23	5	3	4	4	76.9 ± 14.9	18.3 ± 1.4	414.0 ± 5.2
BXD24	4	4	4	4	113.6 ± 14.0	25.8 ± 1.9	408.1 ± 3.9
BXD25	4	4	5	3	61.5 ± 6.8	15.7 ± 1.3	391.9 ± 9.8
BXD27	2	6	4	4	126.8 ± 24.2	23.5 ± 2.3	358.0 ± 4.9
BXD28	5	3	4	4	76.9 ± 8.5	21.3 ± 1.3	395.4 ± 4.7
BXD29	1	7	5	3	72.8 ± 11.2	16.9 ± 1.5	371.1 ± 9.2
BXD30	4	3	4	3	91.0 ± 20.6	18.2 ± 1.5	361.2 ± 11.4
BXD40	5	3	4	4	51.3 ± 2.6	18.5 ± 1.3	429.7 ± 4.7
BXD31	2	4	3	3	93.5 ± 12.9	22.0 ± 3.2	402.2 ± 11.4
BXD32	3	5	3	5	136.4 ± 36.6	25.3 ± 1.8	446.0 ± 6.6
BXD33	6	2	4	4	54.3 ± 4.1	20.5 ± 1.1	429.2 ± 6.4
BXD34	7	1	4	4	52.9 ± 0.5	23.5 ± 0.5	413.5 ± 5.7
BXD35	4	4	4	4	52.6 ± 0.8	19.9 ± 0.9	410.0 ± 5.8
BXD36	4	4	4	4	83.6 ± 28.2	19.7 ± 2.2	409.3 ± 7.4
BXD38	4	2	3	3	54.2 ± 3.0	20.2 ± 1.4	415.6 ± 5.9
BXD39	6	2	4	4	42.8 ± 1.8	18.5 ± 1.1	396.6 ± 7.8
BXD42	5	3	4	4	51.5 ± 2.9	21.2 ± 0.8	454.5 ± 5.4
Average	4.0	3.4	3.6	3.9	96.0 ± 16.3	22.2 ± 1.5	423.1 ± 6.7
Average (no parentals)	3.9	3.4	3.7	3.8	88.3 ± 14.8	21.9 ± 1.5	422.1 ± 6.8

Values are given as average ± standard error.

volume, 4.7% in dentate gyrus volume, 7.8% in pyramidal cell layer volume and 10.7% in granule cell layer volume (Gurland & Tripathi 1971 correction; Sokal & Rohlf 1995). The apparent increase in the CV is actually a well known trend that arises as a result of increased technical error when measuring progressively smaller structures (Lynch & Walsh 1998). It is therefore likely that the CVs for all parts of the hippocampus are close to, and probably lower than, our estimate of 3.4%. The mean volumes of right and left across all cases differ by only 0.09 mm^3 in hippocampal proper volume and less than 0.01 mm^3 in all other regions. None of these small differences between the right and left side are statistically significant. Thus, we do not detect any significant systematic group asymmetry.

Cell number and granule, pyramidal cell layer volumes

We determined the correlation between cell number and volume for our two smallest structures, the pyramidal cell layer and granule cell layer of the dentate gyrus. In both cases, there was a strong, significant correlation of 0.89 between the two measures. However, in the hippocampus proper and dentate gyrus as a whole, this relationship may vary.

Heritability of hippocampal volume variation

We computed heritability for original values and regression corrected volumes of all parts of the hippocampus. Broad-sense heritability computed using the method of Hegmann and Possidente (1981) ranges from 32 to 42% for variation in hippocampal proper volume, from 26 to 40% for variation in dentate gyrus volume, from 16 to 18% for variation in pyramidal cell layer volume and from 26 to 31% for variation in granule cell layer volume. The decrease in heritability as a function of the decreasing size of each structure reflects the increased fraction of technical error in the total variance of each trait. Thus, it is again likely that the actual heritability of all structures, if they could be measured without error, would be between 25 and 50%.

QTL modulating body weight and brain weight

It is important to establish that our hippocampal volume QTL do not merely represent variation in the correlated traits of brain weight and body weight. To address this question we mapped QTL for these traits (Fig. 2) using WebQTL. Using data gathered in this study (Table 2) we noted suggestive body weight QTL on Chr 7 and nearly suggestive QTL on Chrs 11 and 16. More complete data sets support the presence of a QTL on Chr 11, though this QTL is distal to *DGVi11a*. There were suggestive brain weight QTL on Chrs 15, 16 and 19. The QTL on Chr 15 is distal, while *HipV15a* is proximal. Overall, there was little overlap with the hippocampal volume QTL discussed below.

Mapping hippocampal QTL using BXD mice

We adjusted our raw hippocampal volume measurements by regression using brain weight as a single predictor. Slope and intercept values are given in Table 3. In order to test whether our modeling methods might have affected the presence and position of identified hippocampal volume QTL, we mapped using both raw data and postmodeling residuals (Fig. 3). Multiple R–squared indicates fair association between the predicted and observed values for the models of total hippocampal volume (0.64), hippocampus proper (0.64), pyramidal cell layer (0.58), dentate gyrus (0.27) and granule cell layer (0.38). The QTL identified and discussed below were consistent with respect to position and were easily identifiable in the raw data traces, though significance levels obviously differed between the two approaches, and in some cases peak position was slightly shifted. We conclude from this that our regression to brain weight, despite potential conservative bias, has not otherwise altered the identified QTL.

QTL modulating hippocampal volume

Hipp1a and *Hipp5a* are two loci described in Lu *et al*. (2001) that have effects on hippocampal weight. A locus largely overlapping the position of *Hipp1a* was also shown to have pointwise significant ($P < 0.05$) effects on the volume of the overall hippocampus, the hippocampus proper and the pyramidal cell layer and granule cell layer, and nearly significant ($P < 0.08$) effects in the dentate gyrus. A locus overlapping *Hipp5a* was present at a pointwise significant level ($P < 0.05$) in all regions, but never reaches a genome-wide suggestive significance. In this report we have also been able to detect a new QTL on Chr 15 (*HippV15a,* Fig. 4(d) shows map for hippocampus proper) that affects total hippocampal volume (LRS = 15.1, genome-wide $P = 0.06$). A 1.76-mm^3 difference in total hippocampal volume characterizes BXD strains with *B/B* ($n = 18$) or *D/D* ($n = 14$) alleles at this locus, and the QTL interval extends from approximately 0–21 cM (or 0–51 Mb).

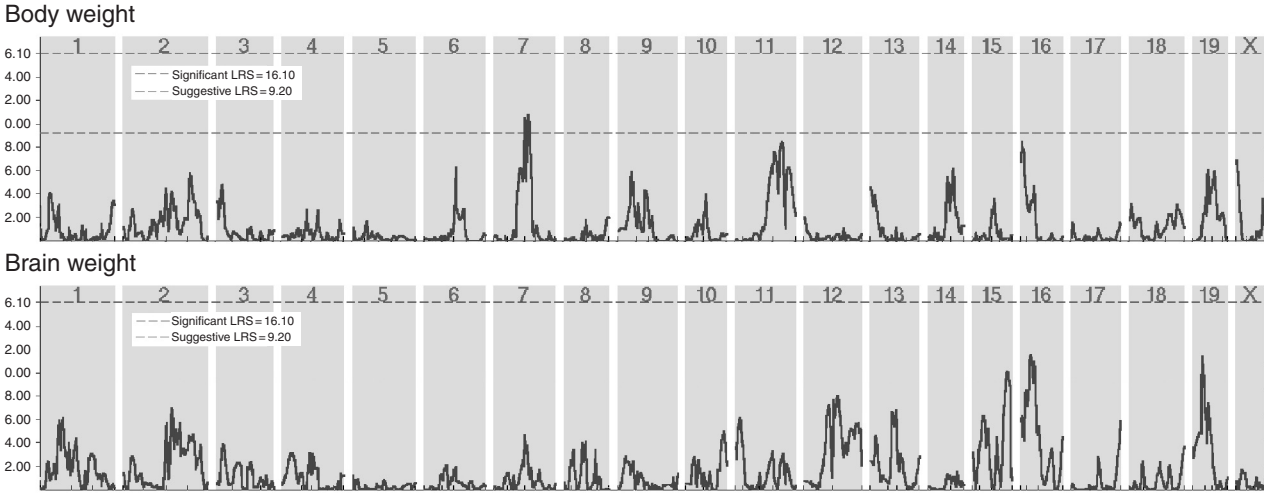

Figure 2: Whole genome interval maps of body weight and brain weight. Maps of these traits demonstrate that brain and body weight QTL are largely different from hippocampus weight QTL. Lower dotted lines represent genome-wide suggestive limit, while upper dotted lines represent cut-off for genome-wide significance.

Table 3: Simple regression of brain weight to volumes of hippocampal regions

Region	Slope per mg brain (wt)	Intercept (mm^3)
Hippocampus	0.055 ± 0.004	0.74 ± 1.75
Hippocampus proper	0.044 ± 0.003	1.09 ± 1.42
Dentate gyrus	0.012 ± 0.001	-0.30 ± 0.44
Pyramidal cell layer	0.0021 ± 0.0004	0.58 ± 0.19
Granule cell layer	0.0019 ± 0.0003	0.063 ± 0.128

Values given in mm^3 as average $\pm$ standard error.

HipV13a, discussed below, also seems to have an effect on total hippocampal volume (point wise $P = 0.006$) but only reaches genome-wide significance in the dentate gyrus. *A* search for two–locus epistatic interactions revealed no significant interaction effects.

QTL modulating volume of the dentate gyrus

In the dentate gyrus, a locus centered near *D13Mit94* (LRS = 17.7; genome-wide $P < 0.05$; Fig. 4(c)) is significant at the genome-wide level by simple interval mapping. Notably, *D13Mit94* also seems to have effects in the hippocampus proper. We therefore conservatively chose to name this locus *HipV13a*. A 0.56-mm^3 difference in dentate gyrus volume characterizes BXD strains with B/B ($n = 14$) or *D/D* ($n = 18$) alleles at this locus, and the QTL interval extends from approximately 26–45 cM (or 42–78 Mb) on Chr 13. Controlling for *HipV13a* in the dentate gyrus reveals suggestive linkage to *D6Mit33*, a marker at the proximal end of Chr 6. Interaction analysis revealed a strong interaction effect between marker *D11Mit78*, located at 2 cM on Chr 11, and *D13Mit91*. From the main effect locus above we know that *D13Mit91* is quite significant by itself. However, individual *t*-tests reveal that D11Mit78 is not significant alone ($P > 0.5$). When *D11Mit78* is *D/D*, there is no detectable effect of *D13Mit91,* while when *D11Mit78* is B/B, *D13Mit91* has a notably stronger effect (Table 4, $P < 0.0001$). The overall effect is significant (genome-wide $P < 0.005$ by permutation analysis), and there was no effect in any other hippocampal region. We therefore named this locus *DGVi11a*.

QTL modulating volume of the granule cell layer of the dentate gyrus

We detected a locus near *D6Mit207* that is suggestive by simple interval mapping and attains genome wide significance when controlling for *D13Mit94* and *D13Mit91* (LRS = 17.5, Fig. 4(b)). This locus overlaps with the suggestive linkage mentioned above. However, when the granule cell layer volume is subtracted from the total dentate gyrus volume, proximal Chr 6 is not at all associated with the remaining volume, suggesting that the granule cell layer may drive the suggestive locus noted above and that this QTL may be specific to the granule cell layer. We named this locus *GrV6a*. A 0.14-mm^3 difference in granule cell layer volume characterizes BXD strains with *B/B* ($n = 19$) or *D/D* ($n = 13$) alleles at this locus, and the QTL interval extends from approximately 7–30 cM (or 29–65 Mb) on Chr 6. A search for two–locus epistatic interactions revealed no significant interaction effects.

QTL modulating volume of the hippocampus proper

HipV15a, discussed earlier, has a strong effect in the hippocampus proper (LRS = 15.1, genome-wide significance $P = 0.06$ by permutation). Additionally, the suggestive hippocampal volume locus overlapping *Hipp1a* (pointwise $P < 0.01$) is also likely to have effects in the hippocampus proper. *HipV15a* does not have strong effects in the dentate gyrus (pointwise $P = 0.07$), suggesting that this QTL may have a more clear effect on the hippocampus proper. However, since the potential effect on the dentate gyrus is near pointwise significance, we did not designate *HipV15a* as specific to the hippocampus proper. A 1.76-mm^3 difference in hippocampus proper volume characterizes BXD strains with *B/B* ($n = 18$) or *D/D* ($n = 14$) alleles at this locus, and the QTL interval extends, as previously mentioned, from approximately 0–21 cM (or 0–51 Mb).

QTL modulating volume of the pyramidal cell layer of the hippocampus proper

In this area, the hippocampal volume locus overlapping *Hipp1a* exceeds the genome-wide suggestive significance level (LRS = 11.8, Fig. 4(a)) by simple interval mapping. This suggestive locus lies between 62 and 91 cM (115–171 Mb). A search for two locus epistatic interactions again revealed no significant interaction effects.

Hippocampus expression profiles

Pavlidis and Noble (2001), in their reanalysis of data generated by Sandberg *et al*. (2000), have demonstrated the tremendous utility of microarray data in winnowing the large number of genes that typically reside in a QTL interval. Sandberg and colleagues used this method to nominate an inwardly rectifying potassium channel (*Kcnj9*) as a potential candidate for an open-field anxiety QTL that also maps very near to *Hipp1a* (Lu *et al*. 2001). We have applied a similar strategy and have identified transcripts that map to 2-LOD support intervals of each QTL and whose forebrain (including hippocampus) expression levels in BXD strains correlate strongly with volume in the hippocampal region affected by that QTL. A selection of these transcripts is listed in Table 5, and additional listings will be made available online.

From 12 422 oligonucleotide probe sets on the Affymetrix short oligonucleotide microarray (Affymetrix U74Av2), a set of transcripts both strongly correlated with the measured traits and located within QTL regions modulating those traits were identified. The transcripts that met both criteria and have a QTL for transcriptional control near their own location are presented as an example of the hypothesis generating

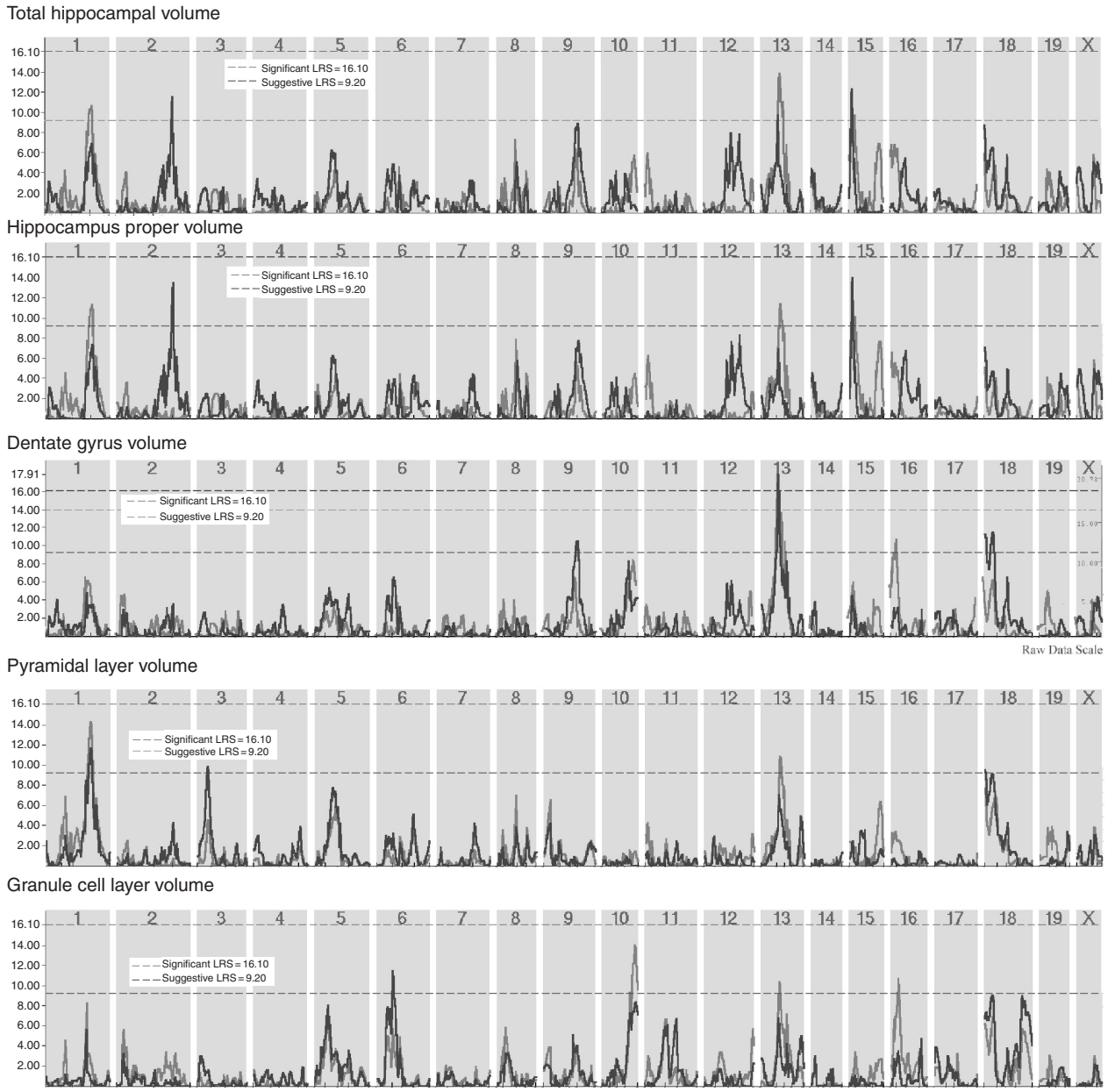

Figure 3: Whole genome interval maps of raw and modeled data. Overlapped maps of raw data (grey lines) and postregression residuals (black lines), demonstrating that our modeling efforts do not broadly affect QTL presence or position. In some cases, the QTL peak is shifted slightly proximally or distally, but the interval of the QTL is not strongly affected. Lower dotted lines represent genome-wide suggestive limit, while upper dotted lines represent cut-off for genome-wide significance, referring in each case to the scale on the left of the graph. Where needed, alternate scales for raw data are presented to the right.

possibilities available to the general community through use of WebQTL and as a nonexclusive starting point for consideration of our identified loci. For instance, because neuron number and thus hippocampal size is regulated primarily by two processes; cell division and cell death, it is interesting to note that several of the highly correlated genes are involved in pathways relevant to these phenomena. However, it is important to remember that this approach will never detect genes whose phenotypic effect does not derive directly from differences in expression.

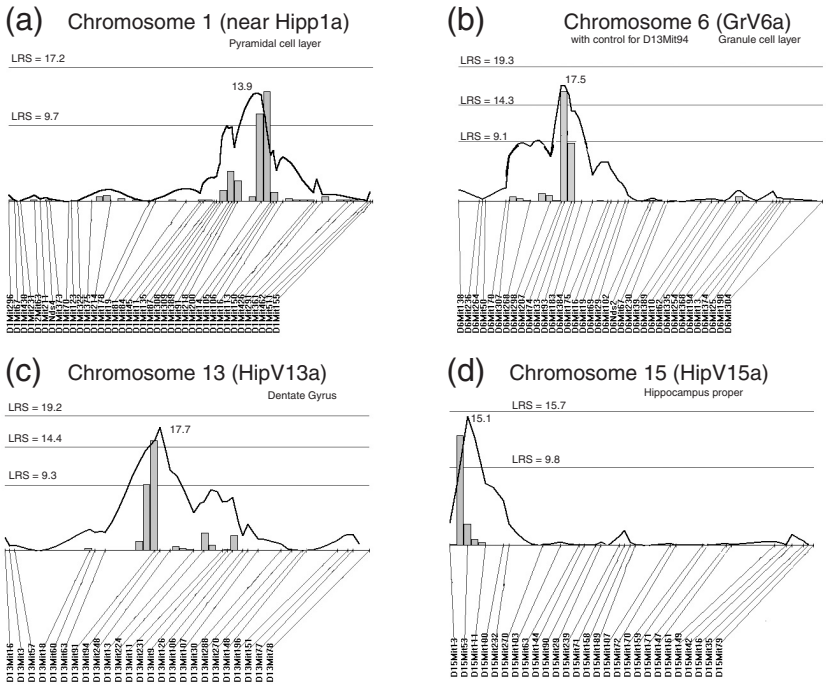

Figure 4: Interval maps of QTL modulating hippocampal volume, generated using QTX. Tissue volume under consideration is noted on the diagram, as is background locus where appropriate. Significance levels were determined by 10 000 permutations. Lowest dotted line represents genome-wide suggestive limit, while upper dotted lines represent cut-off for genome-wide significance and genome-wide high significance, respectively.

Discussion

Synopsis

Differences in the size of the hippocampus in rodents (Jacobs *et al*. 1990; Sherry *et al*. 1992) and humans (Maguire *et al*. 2000) have been shown to relate to differences in functional and behavioral performance including, most prominently, declarative memory formation and navigational skill. Given the wide variety of hippocampus-dependent traits, the gene loci that we have mapped in this study are likely to have interesting behavioral consequences. We have mapped QTL that have pronounced effects on volumes of different regions of the mouse hippocampus to Chr 13 (hippocampus proper and dentate gyrus), Chr 11 (an epistatic interaction effect on the dentate gyrus), Chr 15 (largely hippocampus proper), Chr 6 (granule cell layer of the dentate gyrus) and Chr 1 (pyramidal cell layer, with smaller effects on all regions). These loci are related to differences in the volumes of the hippocampal regions after statistically controlling for background variation in brain size. The selective effects of these QTL, particularly the effect of *GrV6a* on the granule cell layer, suggests that the underlying genes may have important roles in allocating resources to particular hippocampal regions. The QTL may also contribute to behavioral variation in the strains of mice. Since many common behavioral tasks such as context dependent fear conditioning and the Morris water maze are dependent on aspects of hippocampal function, QTL affecting the regions that underlie particular functions may play important roles in determining behavioral phenotypes.

Table 4: Effects of DGVi11a and HipV13a by genotype on dentate gyrus volume

	D11Mit78 B/B	D11Mit78 D/D
D13Mit94 B/B	$0.57 \pm 0.26\,mm^3$, $n = 6$	$0.06 \pm 0.16\,mm^3$, $n = 9$
D13Mit94 D/D	$-0.42 \pm 0.36\,mm^3$, $n = 11$	$-0.07 \pm 0.17\,mm^3$, $n = 8$

Residuals applicable to each combination of genotype.

Specificity of QTL effects

The most direct approach to identifying QTL modulating the volumes of these hippocampal regions would be to measure the volumes in each strain and perform a straightforward QTL analysis on these primary measurements. Unfortunately, this approach does not distinguish between QTL with effects specific to the relative size of hippocampal structures and QTL with global effects on correlated measures such as body weight and brain weight. In order to increase our ability to distinguish QTL selectively modulating the volume of hippocampal structures, we performed a simple regression using

Table 5: Selected brain transcripts highly correlated with BXD hippocampal volume

Chr	Symbol	Description	Chr:MB Position*	Phenotype correlation†
Chr 1	Rgs16	Regulator of G-protein signaling 16	1:154.69	0.3703
Suggestive	Astn1	Astrotactin	1:159.817	0.3711
Locus	Gas5	Growth arrest specific 5	1:159.817	0.3711
	Hoxa4	Homeobox A4	6:52.58	−0.3160
GrV6a	Sec8	Secretory binding protein 8 (S. cerevisiae) homolog	6:34.09	0.4102
	Cai	Calcium binding protein, intestinal	6:48124	0.3835
HipV13a	Bmp6	Bone morphogenesis protein 6	13:27.901	0.4688
	Tpmt	Thiopurine methyltransferase	13:46.666	−0.4004
HipV15a	Gdnf	Glial cell line-derived neurotrophic factor	15:7.66	0.3656

*Chromosomal and megabase location of transcript based on BLAT search of mouse genome (database) for Affymetrix probe sequence.
†Spearman's rank correlation of hippocampal phenotypes with expression of transcripts in BXD mouse brain.

the largest confounding factor; brain weight, and mapped QTL using the residuals. We verified that this did not significantly change the nature of our QTL by comparing these maps to those generated using the raw hippocampal volumes. In nearly all cases the positions of QTL effects were very similar, though a suggestive QTL appears on Chr 2 in the modeled data only. Because this peak is inconsistent and does not achieve genome-wide significance, we make no claims for its interpretation. We also mapped QTL for body weight and brain weight directly and verified that QTL defined by these phenotypes do not significantly overlap with those related to hippocampal volume in our population.

However, the problem of excluding genes with widespread effects on CNS structures is still difficult, because QTL can often have pleiotropic and differential effects on many brain regions and cell types. Such genes may be correctly considered to be hippocampal region-specific QTL if their effect on one or more hippocampal regions is significantly different from their effects on other regions. The inclusion of brain volume in our region-specific models removes some of these effects, but does not fully address situations in which the relative volumes of multiple CNS structures are affected. So, while we have attempted to define the specificity of QTL action with respect to overall brain volume and volume of the examined hippocampal regions, we cannot exclude the possibility that these QTL have effects on the relative volumes of other CNS structures. One of the advantages of using RI strains is that this is a solvable problem. The BXD animals described here have also been used to study the cerebellum (Airey *et al*. 2001), thalamus (Kulkarni *et al*. 2000) and the olfactory bulb (Williams *et al*. 2001b). As previously mentioned, BXDs have also been used to define *Hipp1a* and *Hipp5a*, QTL modulating hippocampal weight (Lu *et al*. 2001), and all of these results can be compared with the current data.

In this study we divided the hippocampus into two major regions: the dentate gyrus and the hippocampus proper. Within these larger regions we also examined the granule cell layer of the dentate gyrus and the pyramidal cell layer of the hippocampus proper. It is reasonable to expect that the control of volume for these hippocampal regions will overlap considerably. However, there is also reason to expect that the overlap will not be complete for all hippocampal subregions, particularly the hippocampus proper and the dentate gyrus. Microarray observations of C57BL/6 animals by Zhao *et al*. (2001) showed that gene expression differs considerably between CA subregions in the hippocampus proper. There were even more expression differences between the hippocampus proper and the dentate gyrus. It is reasonable to assume, especially given the extensive neurogenesis specific to the dentate gyrus, that some of these expression differences will be relevant to the regional volume phenotypes. This expectation is particularly met with respect to *GrV6a*, which has volume effects undetected in regions other than the granule cell layer of the dentate gyrus.

QTL that influence the volume of particular hippocampal regions may be powerful tools for studying structure-function correlations. However, since a typical QTL spans approximately 2% of the genome, it is unwise to confidently conclude that colocalized QTL represent the same underlying gene without significant fine mapping or additional indications (such as the high correlation of hippocampal volume and weight (Lu *et al*. 2001) with respect to the overlap of *Hipp1a* and the suggestive pyramidal cell layer volume QTL defined here). The correlation of these traits indicates that they do share common genetic determinants. Ultimately it will be important to fine map QTL to 1–2 Mb intervals by various means (Darvasi 1998; Hitzemann *et al*. 2002; Williams *et al*. 2001c) to differentiate between QTL that overlap by chance and QTL that share the same underlying genetic basis. It is also worth noting that the QTL discussed here are currently defined only in the context of a B6 × D2 cross. It might be valuable to apply multiple cross mapping (Hitzemann *et al*. 2002) or a similar technique to determine whether the genetic influences noted here remain consistent in various backgrounds. As Hitzemann and colleagues observe, such crosses can also be used to considerably

refine QTL map positions by considering inbred strain haplotypes in the QTL interval.

Effects of hippocampal region QTL

We are ultimately interested in determining the molecular, cellular and behavioral significance of differences in the volume of hippocampal regions. Recombinant inbred strains are a particularly good model in which to investigate such potentially correlated measures, because numerous investigators can study related traits and QTL in genetically identical cohorts. This can be useful in understanding the potentially widespread effect of a QTL identified in a particular context. For instance, Lassalle *et al*. (1999) analyzed the mossy fiber projection system of the hippocampus in 26 BXD strains. This projection system originates from the large population of glutamatergic granule cells of the dentate gyrus and projects primarily to the pyramidal cells of the CA_3 region (reviewed in Henze *et al*. 2000). Interestingly, their measurement of total mossy fiber area correlates positively with total hippocampal weight ($r = 0.54$) and Lasalle and coworkers identified a region on distal Chr 1 associated with total mossy fiber area. Since this QTL overlaps *Hipp1a*, which has broad effects on hippocampus volume and weight, it is likely that the increase in mossy fiber area is a consequence of a general increase in hippocampal size. The possibility that these QTL are the same affects our assumptions in the search for candidate genes underlying QTL effect. This same correlation analysis becomes quite powerful when combined with large microarray and proteomic data sets. Variation in the volume of the hippocampus correlates well with variation in expression of a number of genes in the QTL intervals.

In addition to suggesting multiple roles for single QTL and identity of overlapping QTL, examining multiple aspects of the hippocampus is also crucial in testing the putative specificity of QTL action. For instance, the specific effect of *GrV6a* on the volume of the granule cell layer and its lack of apparent effects in other regions suggests that *GrV6a* may have an unusually intense or restricted effect on granule cell proliferation or maturation. Additional data about range of effects and QTL interactions, such as that between *HipV13a* and *DGVi11a,* can also potentially provide important clues about the nature of a pair of loci, thereby constraining the eventual consideration of candidates and focusing follow-up studies on the most likely genes.

The uniquely replicable nature of RI phenotypes also allows us to speculate on common effects by examining the correlations between our hippocampal volume phenotypes and other physiological and behavioral characteristics that have been examined in the BXD RI strain set. This process is greatly facilitated by the extensive collection of RI phenotypes whose correlations with new phenotypes can be easily examined in WebQTL. A quick perusal of the highest correlations between our volume phenotypes and published phenotypes shows a strong correlation ($r = 0.58$, comparison-wise $P < 0.003$, $n = 23$) between dentate gyrus volume and inhibition of the acoustic startle response caused by application of a 110-db, 10 kHz tone (McCaughran *et al*. 1999). Since acoustic startle is inversely related to proliferation of granule cells in the dentate gyrus (Mickley & Ferguson 1989) and transient disruption of hippocampal activity reduces prepulse inhibition of acoustic startle (Zhang *et al*. 2002), it is reasonable to suppose that hippocampal volume, particularly of the dentate gyrus and included granule cell layer ($r = 0.58$, $P = 0.003$, $n = 23$), are related to this behavioral phenotype. Notably, volume of the pyramidal cell layer of the hippocampus proper is also slightly less strongly correlated,($r = 0.51$, $P = 0.01$, $n = 23$) while the hippocampus proper correlation just misses significance ($r = 0.38$, $P = 0.07$, $n = 23$).

Genes in the QTL interval

In the absence of compelling candidates and convincing auxiliary biological data, it is difficult to make a definitive case for particular candidate genes in the large intervals that define typical QTL. Our ultimate approach to this problem will be to fine map each QTL to a much smaller interval. Here, however, we briefly consider the types of genes in the QTL interval that may be of potential interest. One such category is genes with varying expression. Using WebQTL, we examined genes that map within our QTL intervals and whose expression pattern in the BXD RI strains correlates strongly with the appropriate regional volume phenotype. Of course, this approach overlooks polymorphic genes with no expression variation. Interestingly, several genes with correlated expression patterns are involved in aspects of oxidative stress and neurogenesis. These themes could affect hippocampal volume, given the variations in cell death (reviewed in Finlay 1992), neuron turnover and environmental responses (Kempermann *et al*. 1997a, b) observed in different regions of the brain. In the short synopses below we consider interesting themes and genes from a variety of sources. It is important to note that this is by no means a comprehensive approach and in no way replaces the requirement for fine mapping.

Suggestive Chr 1 locus overlapping Hipp1a

Hipp1a was defined as a hippocampal weight QTL with broad effects on hippocampal volume (Lu *et al*. 2001) which are confirmed in this analysis. Criteria are similar for interesting genes mapping to this locus and *Hipp1a*, since a common factor could generate effects on both volume and weight. Lu and colleagues discussed the retinoid × receptor gamma (*Rxrg*) gene (88 cM on Chr 1) because *Rxrg* affects hippocampal development, is expressed in the adult hippocampus (Zetterstrom *et al*. 1999) and compromises hippocampus-dependent maze learning when absent (*Rxrg* knockout mice, Chiang *et al*. 1998). There is a moderate correlation ($r = 0.29$) between *Rxrg* and dentate gyrus volume, as well as a lower ($r = 0.21$) correlation with total

hippocampal volume, though neither met criteria for inclusion in Table 5.

HipV13a

HipV13a's effects are notable in the dentate gyrus, which experiences continuous generation of new neurons and other cells. According to Kempermann *et al*. (1997a) most mouse strains produced approximately 0.3% of their granule cells as new neurons over a 6-day period. Kempermann and colleagues also observed that B6 mice experienced significantly more granule cell proliferation than CD1, 129/SvJ and BALB/c, and observed in a later study (Kempermann *et al*. 2002a) that D2 has a comparatively low level of neurogenesis. Environment also significantly influences hippocampal neurogenesis (Kempermann *et al*. 1997b; Kempermann & Gage 2002; others) suggesting that genes involved in responses to environmental stimuli might also be interesting candidates for *HipV13a*.

HipV15a

Glial cell line-derived neurotrophic factor (*Gdnf*) is strongly correlated with volume of the hippocampus proper and maps in the *HipV15a* interval. The growth hormone receptor, *Ghr* (Chr 15 at 3.1Mb) is also interesting, though its expression is not strongly correlated with volume phenotypes. Dentate gyrus *Ghr* expression is initially down-regulated and then up-regulated in response to restraint stress in water, down-regulated by adrenalectomy and up-regulated by dexamethasone (Fujikawa *et al.* 2000). As Fujikawa and colleagues speculate, this may indicate that *Ghr* expression is responsive to ACTH and glucocorticoid levels. Since stress affects hippocampal neurogenesis (reviewed in Gould *et al*. 2000) *Ghr* could be involved in stress-response related changes in hippocampal volume.

GrV6a

One strongly correlated gene in the *GrV6a* interval is homeobox A4 (*Hoxa4*). Other Hox genes in the closely linked cluster on Chr 6 are also correlated with granule layer volume. According to our array data, *Hoxa5*, for instance, is also expressed in the hippocampus, and is known to be expressed in a number of adult neuronal cell types including Purkinje neurons in the cerebellum, and pyramidal and dentate neurons in the hippocampus (Odenwald *et al*. 1987). *Npy* is also an interesting candidate, as it is known to reduce behavioral stress responses in a variety of model systems including rats overexpressing *Npy* in the hippocampus (Thorsell *et al*. 2000) and, as previously mentioned, stress is inversely proportional to the generation of new cells in the dentate gyrus (reviewed in McEwen 1999; Gould *et al*. 2000).

Hippocampal size and sex differences

In this paper we have identified significant differences in hippocampal size between males and females, despite a lack of significant differences in the overall volume of male and female brains. Consistent with earlier literature, sex differences in hippocampal size parameters are subtle, strain specific and tending in the direction of males having larger hippocampi than females. Males in this study were found to have a larger hippocampus proper, dentate gyrus and granule cell layer. These sex differences may be attributable to the increase typically observed in the male rodent hippocampus (for review see Madeira & Lieberman 1995), or to increased dendritic field arborization found in males reared in typical laboratory cages (Gould *et al*. 1990; Juraska 1991). The observed sex difference, both on an absolute and relative basis, is fairly small, constituting only about 2% of the total variation in hippocampal volumes. However it does confirm the differences observed by Lu *et al*. (2001) as well as the larger differences found in other species of rodent. For instance, polygamous male voles (Jacobs *et al*. 1990) and kangarooo rats (Jacobs *et al*. 1994) – species that may often travel large distances in search of mates – have hippocampi 10–15% larger than their female counterparts, an increase that correlates with superior spatial ability (Jacobs *et al*. 1990; Sherry *et al*. 1992). The sex-specific hippocampal volume differences in laboratory mice are much smaller and, like the weight differences discussed previously (Lu *et al*. 2001), and do not constitute a strong sexual dimorphism.

Conclusion

Our identification of novel hippocampal volume QTL with possible regional specificity adds significantly to our understanding of the genetic basis of variation in hippocampal structures, and has allowed us to identify loci which determine both general and trait specific aspects of morphology. The substantial evidence for genetic relationships between hippocampal structure and aspects of learning and memory (Crusio *et al*. 1993; Lipp *et al*. 1989; Upchurch & Wehner 1989; and others) and the evidence for behavioral differences due to changes in the relative sizes of hippocampal structures (Roullet & Lassalle 1990; reviewed in Crusio 2001) suggest that these variations may well have effects on numerous hippocampus-dependent tasks. QTL that we have begun to map and characterize are therefore likely to have detectable behavioral consequences in addition to their direct effect on morphology. In addition to fine mapping these novel QTL (an arduous and ongoing effort) we will attempt to identify functional differences in behavioral and cell biology with similar underlying maps by various means, including additional RI and RIX mapping (Williams *et al*. 2001c) and expression profiling specific to the hippocampus.

References

Abusaad, I., MacKay, D., Zhao, J., Stanford, P., Collier, D.A. & Everall, I.P. (1999) Stereological estimation of the total number of neurons in the murine hippocampus using the optical disector. *J Comp Neurol* **408**, 560–566.

Airey, D.C., Lu, L. & Williams, R.W. (2001) Genetic control of the mouse cerebellum: identification of quantitative trait loci modulating size and architecture. *J Neurosci* **21**, 5099–5109.

Chiang, M.Y., Misner, D., Kempermann, G., Schikorski, T., Giguere, V., Sucov, H.M., Gage, F.H., Stevens, C.F. & Evans, R.M. (1998) An essential role for retinoid receptors RARβ and RXRγ in long-term potentiation and depression. *Neuron* **21**, 1353–1361.

Churchill, G.A. & Doerge, R.W. (1994) Empirical threshold values for quantitative trait mapping. *Genetics* **138**, 963–971.

Crusio, W.E. (2001) Genetic dissection of mouse exploratory behavior. *Behav Brain Res* **125**, 127–132.

Crusio, W.E., Schwegler, H. & Brust, I. (1993) Covariations between hippocampal mossy fibres and working and reference memory in spatial and non-spatial radial maze tasks in mice. *Eur J Neurosci* **5**, 1413–1420.

Darlington, R.B. & Smulders, T.V. (2001) Problems with residual analysis. *Anim Behav* **62**, 599–602.

Darvasi, A. (1998) Experimental strategies for the genetic dissection of complex traits in animals. *Nat General* **18**, 19–24.

Deadwyler, S.A., Foster, T.C. & Hampson, R.E. (1987) Processing of sensory information in the hippocampus. *CRC Crit Rev Clin Neurobiol* **2**, 335–355.

Finlay, B.L. (1992) Cell death and the creation of region differences in neuronal numbers. *J Neurobiol* **23**, 1159–1171.

Fujikawa, T., Soya, H., Fukuoka, H., Alam, K.S., Yoshizato, H., McEwen, B.S. & Nakashima, K. (2000) A biphasic regulation of receptor mRNA expressions for growth hormone, glucocorticoid and mineralocorticoid in the rat dentate gyrus during acute stress. *Brain Res* **874**, 186–193.

Gass, P., Wolfer, D.P., Balschun, D., Rudolph, D., Frey, U., Lipp, H.P. & Schutz, G. (1998) Deficits in memory tasks of mice with CREB mutations depend on gene dosage. *Learn Mem* **5**, 274–288.

Gould, E., Tanapat, P., Rydel, T. & Hastings, N. (2000) Regulation of hippocampal neurogenesis in adulthood. *Biol Psychiatry* **48**, 715–720.

Gould, E., Westlind-Danielsson, A., Frankfurt, M. & McEwen, B.S. (1990) Sex differences and thyroid hormone sensitivity of hippocampal pyramidal cells. *J Neurosci* **10**, 996–1003.

Graves, L., Dalvi, A., Lucki, I., Blendy, J.A. & Abel, T. (2002) Behavioral analysis of CREB alphadelta mutation on a B6/129, F1 hybrid background. *Hippocampus* **12**, 18–26.

Gurland, J. & Tripathi, R.C. (1971) A simple approximation for unbiased estimation of the standard deviation. *Amer Stat* **25**, 30–32.

Haley, C.S. & Knott, S.A. (1992) A simple regression method for mapping quantitative trait loci in line crosses using flanking markers. *Heredity* **69**, 315–324.

Hegmann, J.P. & Possidente, B. (1981) Estimating genetic correlations from inbred strains. *Behav Genet* **11**, 103–114.

Henze, D.A., Urban, N.N. & Barrionuevo, G. (2000) The multifarious hippocampal mossy fiber pathway: a review. *Neuroscience* **98**, 407–427.

Hitzemann, R., Balmanger, B., Cooper, S., Coulombe, S., Reed, C., Demarest, K., Joyner, K., Cipp, L., Flint, J., Talbot, C., Rademacher, B., Buck, K. & McCaughran, J. Jr (2002) Multiple Cross Mapping (MCM) markedly improves the localization of a QTL for ethanol iduced activation. *Genes, Brain, Behavior* **1**, 214–222.

Jacobs, L.F., Gaulin, S.J.C., Sherry, D.F. & Hoffman, G.E. (1990) Evolution of spatial cognition: sex-specific patterns of spatial behavior predict hippocampal size. *Proc Natl Acad Sci USA* **87**, 6349–6352.

Jacobs, L.F. & Spencer, W.D. (1994) Natural space-use patterns and hippocampal size in kangaroo rats. *Brain Behav Evol* **44**, 125–132.

Juraska, J.M. (1991) Sex differences in 'cognitive' regions of the rat brain. *Psychoneuroendocrinology* **16**, 105–119.

Kempermann, G. & Gage, F.H. (2002) Genetic influence on phenotypic differentiation in adult hippocampal neurogenesis. *Dev Brain Res* **134**, 1–12.

Kempermann, G., Kuhn, H.G. & Gage, F.H. (1997a) Genetic influence on neurogenesis in the dentate gyrus of adult mice. *Proc Natl Acad Sci USA* **94**, 10 409–10 414.

Kempermann, G., Kuhn, H.G. & Gage, F.H. (1997b) More hippocampal neurons in adult mice living in an enriched environment. *Nature* **386**, 493–495.

Kesner, R.P., Gilbert, P.E. & Wallenstein, G.V. (2000) Testing neural network models of memory with behavioral experiments. *Curr Opin Neurobiol* **10**, 260–265.

Kulkarni, A., Airey, D.C. & Williams, R.W. (2000) Genetic architecture of the mouse retinogeniculate system: a QTL analysis of numerical matching. *Soc Neurosci Abstract* **26**, 1087.

Lassalle, J.M., Halley, H., Milhaud, J.M. & Roullet, P. (1999) Genetic architecture of the hippocampus mossy fiber subfields in the BXD RI mouse strain series: a preliminary QTL analysis. *Behav Genet* **29**, 273–282.

Lipp, H.P., Schwegler, H., Crusio, W.E., Wolfer, D.P., Leisinger-Trigona, M.C., Heimrich, B. & Driscoll, P. (1989) Using genetically-defined rodent strains for the identification of hippocampal traits relevant for two-way avoidance behavior: a non-invasive approach. *Experientia* **45**, 845–859.

Lu, L., Airey, D.C. & Williams, R.W. (2001) Complex trait analysis of the hippocampus: Mapping and biometric analysis of two novel gene loci with specific effects on hippocampal structure in mice. *J Neurosci* **21**, 3503–3514.

Lynch, M. & Walsh, B. (1998) *Genetics and Analysis of Quantitative Traits*. Sinauer, Sunderland, MA.

Madeira, M.D. & Lieberman, A.R. (1995) Sexual dimorphism in the mammalian limbic system. *Prog Neurobiol* **45**, 275–333.

Maguire, E.A., Gadian, D.G., Johnsrude, I.S., Good, C.D., Ashburner, J., Frackowiak, R.S. & Frith, C.D. (2000) Navigation-related structural change in the hippocampi of taxi drivers. *Proc Natl Acad Sci USA* **97**, 4414–4416.

Manly, K.F., Cudmore, R.H. Jr & Meer, J.M. (2001) Map Manager QTX, cross-platform software for genetic mapping. *Mammalian Genome* **12**, 930–932.

McCaughran, J. Jr, Bell, J. & Hitzemann, R. (1999) On the relationships of high-frequency hearing loss and cochlear pathology to the acoustic startle response (ASR) and prepulse inhibition of the ASR in the BXD recombinant inbred series. *Behav Genet* **29**, 21–30.

McEwen, B.S. (1999) Stress and hippocampal plasticity. *Annu Rev Neurosci* **22**, 105–122.

Mickley, G.A. & Ferguson, J.L. (1989) Enhanced acoustic startle responding in rats with radiation-induced hippocampal granule cell hypoplasia. *Exp Brain Res* **75**, 28–34.

Odenwald, W.F., Taylor, C.F., Palmer-Hill, F.J., Friedrich, V. Jr, Tani, M. & Lazzarini, R.A. (1987) Expression of a homeo domain protein in noncontact-inhibited cultured cells and postmitotic neurons. *Genes Dev* **1**, 482–496.

Pavlidis, P. & Noble, W.S. (2001) Analysis of strain and regional variation in gene expression in mouse brain. *Genome Biol* **2**, RESEARCH0042.

Roullet, P. & Lassalle, J.M. (1990) Genetic variation, hippocampal mossy fibers distribution, novelty reactions and spatial representation in mice. *Behav Brain Res* **41**, 61–69.

Ruberti, F., Capsoni, S., Comparini, A., Di Daniel, E., Franzot, J., Gonfloni, S., Rossi, G., Berardi, N. & Cattaneo, A. (2000) Phenotypic knockout of nerve growth factor in adult transgenic mice reveals severe deficits in basal forebrain cholinergic neurons, cell death in the spleen, and skeletal muscle dystrophy. *J Neurosci* **20**, 2589–2601.

Sandberg, R., Yasuda, R., Pankratz, D.G., Carter, T.A., Del Rio, J.A., Wodicka, L., Mayford, M., Lockhart, D.J. & Barlow, C. (2000) Regional and strain-specific gene expression mapping in the adult mouse brain. *Proc Natl Acad Sci USA* **97**, 11 038–11 043.

Shapiro, M. (2001) Plasticity, hippocampal place cells, and cognitive maps. *Arch Neurol* **58**, 874–881.

Sherry, D.F., Jacobs, L.F. & Gaulin, S.J. (1992) Spatial memory and adaptive specialization of the hippocampus. *Trends Neurosci* **15**, 298–303.

Shou, S., Lu, L., Qu, Y., Jensen, P. & Williams, R.W. (2002) High transcriptional diversity and complexity among mouse brain regions. *Soc Neurosci Abstract Program* **no**. **903**.**8**.

Sokal, R.R. & Rohlf, F.J. (1995) *Biometry: the Principles and Practice of Statistics in Biological Research*, 3rd edn. W.H. Freeman, New York.

Taylor, B.A. (1989) Recombinant inbred strains. In Lyon, M.L. & Searle, A.G. (eds), *Genetic Variants and Strains of the Laboratory Mouse*, 2nd edn. Oxford UP, Oxford, pp. 773–796.

Taylor, B.A., Wnek, C., Kotlus, B.S., Roemer, N., MacTaggart, T. & Phillips, S.J. (1999) Genotyping new BXD recombinant inbred mouse strains and comparison of BXD and consensus maps. *Mamm Genome* **10**, 335–348.

Thorsell, A., Michalkiewicz, M., Dumont, Y., Quirion, R., Caberlotto, L., Rimondini, R., Mathe, A.A. & Heilig, M. (2000) Behavioral insensitivity to restraint stress, absent fear suppression of behavior and impaired spatial learning in transgenic rats with hippocampal neuropeptide Y overexpression. *Proc Natl Acad Sci USA* **97**, 12 852–12 857.

Upchurch, M. & Wehner, J.M. (1989) Inheritance of spatial learning ability in inbred mice: a classical genetic analysis. *Behav Neurosci* **103**, 1251–1258.

Wang, J., Williams, R.W., Chesler, E.J. & Manly, K.F. WebQTL: Web-based complex trait analysis. *Neuroinformatics* in press.

Williams, R.W. (2000) Mapping genes that modulate mouse brain development: a quantitative genetic approach. In Goffinet, A. & Rakic, P. (eds), *Mouse Brain Development*. Springer, Berlin, pp. 21–49.

Williams, R.W., Airey, D.C., Kulkarni, A., Zhou, G. & Lu, L. (2001b) Genetic dissection of the olfactory bulbs of mice: QTLs on four chromosomes modulate bulb size. *Behav Genet* **1**, 61–77.

Williams, R.W., Gu, J., Qi, S. & Lu, L. (2001a) The genetic structure of recombinant inbred mice: high-resolution consensus maps for complex trait analysis. *Genome Biol* **2**, RESEARCH0046.

Williams, R.W., Manly, K.F., Shou, S., Chesler, E., Hsu, H.C., Mountz, J., Wang, J., Threadgill, D.W. & Lu, L. (2002) Massively parallel complex trait analysis of transcriptional activity in mouse brain. *Int Mouse Genome Conf* **16**, 46.

Williams, R.W., Threadgill, D.W., Manly, K.F., Rosen, G.D., Shou, S., Airey, D.C., Gu, J. & Lu, L. (2001c) *Integrated complex trait analysis of brain and behavior in mouse: near-term prospects for high-resolution QTL mapping using large RI and RIX sets*. The 4th Annual Meeting of the International Behavioural and Neural Genetics Society*, San Diego, USA, November 8–10, 2001*.

Wimer, C.C. & Wimer, R.E. (1989) On the sources of strain and sex differences in granule cell number in the dentate area of house mice. *Brain Res Dev Brain Res* **48**, 167–176.

Wimer, R.E. & Wimer, C. (1985) Three sex dimorphisms in the granule cell layer of the hippocampus in house mice. *Brain Res* **328**, 105–109.

Wimer, R.E., Wimer, C.C., Vaughn, J.E., Barber, R.P., Balvanz, B.A. & Chernow, C.R. (1976) The genetic organization of neuron number in Ammon's horns of house mice. *Brain Res* **118**, 219–243.

Wimer, R.E., Wimer, C.C., Vaughn, J.E., Barber, R.P., Balvanz, B.A. & Chernow, C.R. (1978) The genetic organization of neuron number in the granule cell layer of the area dentata in house mice. *Brain Res* **157**, 105–122.

Wittenberg, G.M. & Tsien, J.Z. (2002) An emerging molecular and cellular framework for memory processing by the hippocampus. *Trends Neurosci* **10**, 501–505.

Zetterstrom, R.H., Lindqvist, E., Urquiza, A.M., Tomac, A., Eriksson, U., Perlmann, T. & Olson, L. (1999) Role of retinoids in the CNS: differential expression of retinoid binding proteins and receptors and evidence for presence of retinoic acid. *Eur J Neurosci* **11**, 407–416.

Zhang, W.N., Bast, T. & Feldon, J. (2002) Prepulse inhibition in rats with temporary inhibition/inactivation of ventral or dorsal hippocampus. *Pharmacol Biochem Behav* **73**, 929–940.

Zhao, X., Lein, E.S., He, A., Smith, S.C., Aston, C. & Gage, F.H. (2001) Transcriptional profiling reveals strict boundaries between hippocampal subregions. *J Comp Neurol* **441**, 187–196.

Acknowledgments

This research project was supported by a grant from the Human Brain Project (MH 62009). The authors thank Drs Guomin Zhou, Jing Gu and Xiyun Peng for their assistance in generating, processing and genotyping F2 and BXD mice. We thank Dr Glenn Rosen for his participation in creating the Mouse Brain Library.